CALIBRATING TRANSPORT LINES USING LOCO TECHNIQUES*

Yves R. Roblin†, TJNAF, Newport News, VA, 23606, USA

Abstract

With the 12GeV upgrade underway at CEBAF, there is a need to recharacterize the beamlines after modifications made to them to accommodate running at higher energies. We present a linear perturbation approach to calibrating the optics model of transport lines. This strategy is adapted from the LOCO method in use for storage rings [1] . We consider the effect of quadrupole errors, dipole construction errors as well as beam position monitors calibrations. The ideal model is expanded to first order in Taylor series of the errors. A set of difference orbits obtained by exciting the correctors along the beamline is taken, yielding the measured response matrix. An iterative procedure is invoked and quadrupole errors as well as beam position monitors (BPM) calibration factors are obtained. Here we present details of the method and results of first measurements at CEBAF from late 2010 and early 2011.

INTRODUCTION

This paper outlines a linear perturbation approach to calibrating the optics model of transport lines. After presenting the algorithm and validation of the method, we discuss the measurements that were taken at Jefferson Lab in late 2010 and early 2011 in preparation of the shutdown for the 12GeV upgrade.

ALGORITHM

We start with the premise that we have a design model $\mathcal{R}$ of the machine. From this model we can compute the response matrix defined as the BPM to corrector coefficients such that $\mathcal{R}_{ij} = \Delta x_i / \Delta x'_j$. Likewise, we can measure this transport matrix in the machine by exciting correctors and reading back deviation at the BPMs. We will denote the measured transfer matrix elements by $\mathcal{M}_{ij}$. Using this definition, the relationship between the measured matrix and the design matrix can then be expressed at first order as:

$$\mathcal{R}_{ij} = \mathcal{M}_{ij} + \sum_{q}^{N_q} \frac{\mathrm{d}\mathcal{R}_{ij}}{\mathrm{d}k_q} \delta k_q + \sum_{k}^{N_b} \delta_{ik} \mathcal{R}_{ij} \delta g_k \qquad (1)$$

Where we included the quadrupole errors δk_q and BPM gain deviations δg_k. δ_{ik} is the Kronecker symbol.

We can write this equation in matrix form :

$$\mathcal{R} - \mathcal{M} = A \Delta_k \qquad (2)$$

where A is a matrix, Δ_k is a vector of length N_q and $\mathcal{R} - \mathcal{M}$ is the difference between the design response matrix and the measured response matrix written as a column vector :

$$A = \underbrace{\left| \begin{array}{ccccccc} \frac{\mathrm{d}\mathcal{R}_{11}}{\mathrm{d}k_1} & \cdots & \frac{\mathrm{d}\mathcal{R}_{11}}{\mathrm{d}k_{N_q}} & \mathcal{R}_{11} & 0 & \cdots & \cdots \\ \frac{\mathrm{d}\mathcal{R}_{12}}{\mathrm{d}k_1} & \cdots & \frac{\mathrm{d}\mathcal{R}_{12}}{\mathrm{d}k_{N_q}} & 0 & \mathcal{R}_{12} & 0 & \cdots \\ \vdots & \vdots & \vdots & \vdots & \vdots & \vdots & \vdots \\ \frac{\mathrm{d}\mathcal{R}_{1N_c}}{\mathrm{d}k_1} & \cdots & \frac{\mathrm{d}\mathcal{R}_{1N_c}}{\mathrm{d}k_{N_q}} & 0 & \cdots & \cdots & \mathcal{R}_{1N_c} \\ \frac{\mathrm{d}\mathcal{R}_{21}}{\mathrm{d}k_1} & \cdots & \frac{\mathrm{d}\mathcal{R}_{21}}{\mathrm{d}k_{N_q}} & \mathcal{R}_{21} & 0 & \cdots & \\ \vdots & \vdots & \vdots & \vdots & \vdots & \vdots & \vdots \\ \frac{\mathrm{d}\mathcal{R}_{N_bN_c}}{\mathrm{d}k_1} & \cdots & \frac{\mathrm{d}\mathcal{R}_{N_bN_c}}{\mathrm{d}k_{N_q}} & 0 & \cdots & \cdots & \mathcal{R}_{N_bN_c} \end{array} \right|}_{N_q+N_b} \updownarrow N_b * N_c$$

$$\mathcal{R} - \mathcal{M} = \left| \begin{array}{c} \mathcal{R}_{11} - \mathcal{M}_{11} \\ \vdots \\ \mathcal{R}_{1N_c} - \mathcal{M}_{1N_c} \\ \mathcal{R}_{21} - \mathcal{M}_{21} \\ \vdots \\ \mathcal{R}_{N_bN_c} - \mathcal{M}_{N_bN_c} \end{array} \right| \quad \Delta_k = \left| \begin{array}{c} \Delta K_1 \\ \vdots \\ \Delta K_{N_q} \end{array} \right|$$

The algorithm is iterative. Firstly, the A matrix is constructed by computing the derivatives of the design response matrix relative to the quadrupole and BPM gain errors. Secondly, The pseudo inverse $A^\dagger = (A^T A^{-1})^{-1} A^T$ is formed and the new Δ_k obtained from $\Delta_k = A^\dagger \mathcal{R}$. Thirdly, the new quadrupole values K_q are updated via $K_q = K_q + \Delta K_q$ and the BPM gains obtained from $g_k = g_k + \Delta g_k$. Finally, the chi-square is computed as $\chi^2 = \|\mathcal{M} - \mathcal{R} - A\Delta_k\|^2$.

The above constitutes one iteration of the algorithm. The procedure is repeated and stops when the desired accuracy is reached, typically indicated by the χ^2 variation falling below a suitable threshold.

RING VERSUS TRANSPORT LINE

In a ring, each corrector kick is felt by every BPM typically resulting in a large number of degrees of freedom. This is what made this method highly successful and allowed for precise determination of the errors.

In the case of a transport line, this situation is not as favorable as BPMs are only sensitive to corrector kicks that are originating upstream. Nevertheless, one can still obtain significantly more equations than unknowns if one exploits the potential symmetries in the optics of the transport line.

In the CEBAF machine, the return arcs are setup as a FODO lattice and require only four unique quadrupole setpoints. By making the assumption that all the quadrupoles

* Work supported by Jefferson Science Associates, LLC under U.S. DOE Contract No. DE-AC05-06OR23177

† roblin@jlab.org

from a same family behave the same way, we drastically reduce the number of unknowns. A fifth gradient assigned to the dipoles is also fitted. Correctors are calibrated separately and are not included in the fitting procedure.

VALIDATION OF THE METHOD BY SIMULATING A MEASUREMENT

We used ELEGANT [2] to compute an ideal design model and to generate a perturbed model in which quadrupole families, dipole body gradient and BPM gains are randomly modified. A C program and a set of perl scripts were written to perform the fitting.

In this model, we assume that all the dipoles have the same systematic quadrupole gradient (body gradient). This results in the fitting being done for these four quadrupole families, the global body gradient and the individual BPM gains.

Table 1 shows an example of convergence from a randomly perturbed model when starting with intrinsic BPMs errors of $200\mu m$.

Including BPM Scale Factors

During the fitting, we also determine the BPM scale factors. We assumed that they are surveyed in such a way that there is no significant rotation of the BPM can (and hence no coupling between X and Y). We observed that within 3 to 4 iterations, the initial random BPM gain distribution is recovered. In practice, we calibrate BPMs externally via injection of a calibrated current and expect a much smaller spread of gains. The fact, that the algorithm works even for grossly miscalibrated BPMs was demonstrated by the numerous random model test fittings we carried out.

After calibration, orbits obtained from the perturbed model are perfectly recovered by the calibrated model as seen in figure 1. We noted that in the case of vertical orbits, the inclusion of the dipole gradient errors is critical to obtain a good fit.

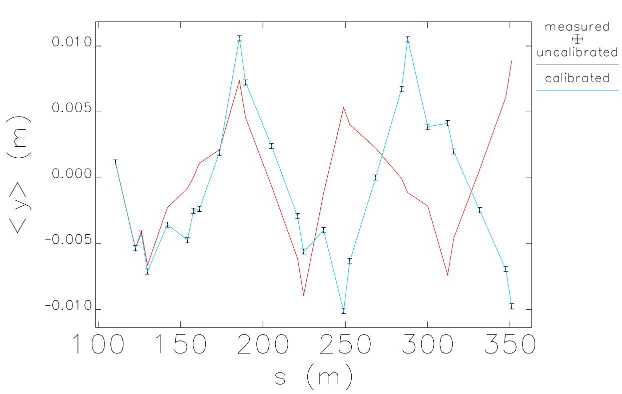

Figure 1: Simulated orbits (points) compared to uncalibrated and calibrated model

Including BPM Resolution

It is possible to perform a weighted least-square fit to include errors at the BPMs. Consider that each bpm has a measurement error σ.

The resulting error on the $\mathcal{M}_{ij}$ response matrix element is therefore $\sigma_{ij} = \frac{\sigma_i}{\Delta\theta}$ where $\Delta\theta$ is the kick in radians.

The A matrix is modified to weight each row by the error computed as described above. We take into account the fact that sigma at the BPMS is heteroscedastic by incorporating the leverage of each BPM in the weighting procedure. The estimator for variance on the fitted variables (quadrupoles and bpm gains) is given by

$$S^2(\Delta) = (A^T A)^{-1} A^T diag(\frac{e_i^2}{(1-h_{ii})^2}) A (A^T A)^{-1} \quad (3)$$

The $\mathcal{R} - \mathcal{M}$ vector is weighted as well. This yields the usual result that the diagonal terms of the covariance matrix give the square of the errors for each fitted parameter.

A standard weighting and weeding of bad bpm is carried out after each iteration where the relative contribution of each BPM to the χ^2 is computed.

WINTER 2010 MEASUREMENTS AT CEBAF

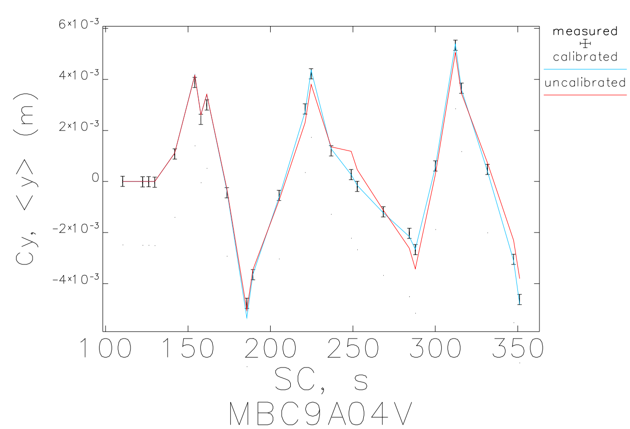

Figure 2: ARC9 measured orbits(points) compared to uncalibrated and calibrated model

Most of the dipole magnets in CEBAF return arcs are being refurbished for the 12 GeV project. Extra return steel is being added to mitigate saturation effects at the higher 12GeV setpoints. During a six month downtime in early 2011, all of these dipoles were removed from the machine, refurbished and then placed back in the tunnel. Prior to removal, data was taken using these LOCO techniques to have a baseline for comparison when recommissioning the upgraded magnets later this fall.

Table 1: Convergence from a random distribution of errors in the model. The first row denotes the perturbed values and the second row shows the fitted values

Δk_1	Δk_2	Δk_3	Δk_4	ΔK_1	χ^2/iter
0.03	-0.01	-0.01	0.022	2e-4	
0.03 ± 1.2e-3	-0.01 ± 2e-3	-0.01 ± 3e-3	0.022 ± 1.6e-3	2e-4 ± 1.6e-4	1.334/19

The data was taken by exciting each corrector in turn and performing differential orbit measurements. Averaging over twenty consecutive BPM measurements as well as taking null kicks and reversed corrector kicks was carried out in order to minimize systematic machine drifts. Defective BPMs were identified at this stage and removed from the analysis. Each data taking session takes about 2 hours for a single return arc.

Starting with our best estimate of the design model, we allowed for fitting of the four quadrupole families, the dipole body gradient and the BPM calibration factors. The procedure converged within a few iterations and yielded results such as shown in Figure 2.

Table 2: Comparison of measured quadrupole and body gradients against values expected from the model for the CEBAF ARC4 return arc. Units are in m^{-2}

Variable	k_1 fitted	k_1 model
A02,A04,..	0.568 ± 1.1e-3	0.569
A03,A07,..	1.003 ± 2.1e-3	0.995
A05,A13,..	0.468 ± 3.0e-3	0.460
A09,A17,..	0.613± 1.6e-3	0.609
Body Gradient	0.0015± 1.4e-4	0.0013

As can be seen from this figure, the design model is already close to what we expect. The most notable deviations occurs in the vertical plane where dipole body gradient is prevalent. In the case of one arc, we did find one quadrupole family signicantly off from expected ; This was traced to a faulty magnetization curve in the control system. We took data for every arc and every corrector.

This fall, during recommissioning of the new dipoles, we will perform these measurements again at 6 GeV. Magnets will not be running with 12GeV settings until 2014 at the earliest and we expect the results to reproduce within a reasonable range in the absence of saturation. Any significant deviation will identify manufacturing or installation problems.

Table 2 is a example of the accuracy of the method shown for the ARC4 return arc. The measured values are found to be within a few part per thousands of the expected values. The sensitivity of this technique to the dipole body gradient is dependent on the strength of the FODO structure. The dipole focusing is weak compared to focusing provided by the main lattice quadrupoles and therefore is difficult to measure accurately.

We estimated the errors by means of a monte-carlo approach where one generates dozens of models with slightly perturbed setpoints relative to the measured setpoints. Error is estimated by the fitting routines and is averaged over many sample trials to give an estimate of the standard deviation of each parameter.

CONCLUSION

We presented an adaptation of the LOCO method routinely employed in circular machines to calibrate the optics model and applied it for the transport lines of the CEBAF accelerator at Jefferson Lab. This method enabled us to baseline the machine in preparation for the 12GeV upgrade. It relies on exploitation of beamline symmetries to reduce the number of unknowns one has to fit. It is often the case that one can prepare a transport line to exhibit this behavior just for the purpose of measurement. Future work will focus on finding the optimal optics configurations for characterizing the magnets in the beamline. Preliminary results are within expectation of the optics models and TOSCA [3] simulations.

REFERENCES

[1] J. Safranek, "Experimental Determination of Storage Ring Optics Using Orbit Response Measurements," *Nucl. Instr. And Meth.* A **388**,27 (1997)

[2] M. Borland, "ELEGANT: A flexible SDDS compliant code for accelerator simulation," APS light source note, **LS287** (2000)

[3] Jay Benesch, *private communication*